

# Finding Complex Patterns in Trajectory Data via Geometric Set Cover

Jacobus Conradi\*

Anne Driemel†

## Abstract

Clustering trajectories is a central challenge when confronted with large amounts of movement data such as full-body motion data or GPS data. We study a clustering problem that can be stated as a geometric set cover problem: Given a polygonal curve of complexity  $n$ , find the smallest number  $k$  of representative trajectories of complexity at most  $l$  such that any point on the input trajectories lies on a subtrajectory of the input that has Fréchet distance at most  $\Delta$  to one of the representative trajectories. This problem was first studied by Akitaya et al. (2021) and Brüning et al. (2022). They present a bicriteria approximation algorithm that returns a set of curves of size  $O(kl \log(kl))$  which covers the input with a radius of  $11\Delta$  in time  $\tilde{O}((kl)^2n + kln^3)$ , where  $k$  is the smallest number of curves of complexity  $l$  needed to cover the input with a distance of  $\Delta$ . The representative trajectories computed by their algorithm are always line segments. In applications however, one is usually interested in representative curves of higher complexity which consist of several edges. We present a new approach that builds upon the works of Brüning et al. (2022) computing a set of curves of size  $O(k \log(n))$  in time  $\tilde{O}(l^2n^4 + kln^4)$  with the same distance guarantee of  $11\Delta$ , where each curve may consist of curves of complexity up to the given complexity parameter  $l$ . To validate our approach, we conduct experiments on different types of real world data: high-dimensional full-body motion data and low-dimensional GPS-tracking data.

---

\*University of Bonn. Partially funded by the Deutsche Forschungsgemeinschaft (DFG, German Research Foundation) - 313421352 (FOR 2535 Anticipating Human Behavior). Affiliated with Lamarr Institute for Machine Learning and Artificial Intelligence.

†Hausdorff Center for Mathematics, University of Bonn, and Lamarr Institute for Machine Learning and Artificial Intelligence.

## 1 Introduction

Advancements in tracking technology made it possible to record large amounts of data ranging through a diverse array of applications from migratory patterns of animals over industrial applications of robots to econometrics. The type of data analyzed in these areas range from GPS-data [24] over complex gestures [22] to full-body motion data [15]. Practitioners are often confronted with vast amounts of data from which one would like to extract a reoccurring pattern, preferably of small complexity. This is of interest when analyzing e.g. full-body motion data in the context of gait analysis [18]. In full-body motion data one would assume there to be a repeated pattern corresponding to the gait of the person being tracked. A particular challenge is identifying the start and end points of such patterns, which is the motivation for algorithms based on heuristics [17]. As the type of pattern which is sought after may vary and thus the quality measurement for a certain pattern varies, there are multiple approaches to tackle this problem (see the survey papers [10, 26, 27]). One quality measure often used in this context is that of the Fréchet distance as a measure of similarity between the given trajectories, examples are the work of Agarwal et al. [1] or that of Buchin et al. [9]. The approach we want to focus on is that of Akitaya et al. [5] who pose the problem as a geometric set cover problem, in which a given trajectory needs to be “covered” by the smallest possible number of “center” trajectories, such that each point of the input trajectory is contained in a subtrajectory of the input trajectory which has a small Fréchet distance to one of the center trajectories. This can similarly be thought of as a clustering problem in which each point on the input trajectory is assigned to at least one center trajectory. One drawback for practical applications of the approaches presented in [5] and the subsequent work of Brüning et al. [4] is that the center trajectories computed only ever consist of a single edge, whereas in applications one is often interested in finding center trajectories of higher complexity, as even a simple circular motion can not be modeled well with a single edge. In this paper we focus on extending the approach of [4] to center trajectories of higher complexity and analyzing our approach on real data.

**1.1 Preliminaries** A *polygonal curve*  $P$  in  $\mathbb{R}^d$  of *complexity*  $n$  is defined by an ordered set of points  $(v_0, \dots, v_n) \subset \mathbb{R}^d$  by concatenating the linear interpolations of consecutive points. That is for each  $1 \leq i \leq n$  we obtain the *edge*  $e_i(t) = (1-t)v_{i-1} + tv_i$  and their concatenation  $e_1 \oplus \dots \oplus e_n : [0, 1] \rightarrow \mathbb{R}^d$  defines  $P$ . We may denote an edge from  $p$  to  $q$  by  $\overline{pq}$ . We denote the set of all polygonal curves in  $\mathbb{R}^d$  of complexity at most  $l \in \mathbb{N}$

by  $\mathbb{X}_l^d$  and the complexity of a polygonal curve  $P$  by  $|P|$ . For a polygonal curve  $P$  and given  $0 \leq s \leq t \leq 1$  we denote the *subcurve* of  $P$  from  $P(s)$  to  $P(t)$  by  $P[s, t]$ . If we drop the requirement that  $s \leq t$ , we say  $P[s, t]$  is a *free subcurve* of  $P$ . A free subcurve of  $P$  is either a subcurve of  $P$  or a subcurve of  $P$  parametrized in the reverse direction.

For two curves in  $\mathbb{R}^d$  their continuous Fréchet distance is defined as

$$d_{\mathcal{F}}(P, Q) = \inf_{f, g} \max_{t \in [0, 1]} \|P(f(t)) - Q(g(t))\|$$

where  $f$  and  $g$  range over all non-decreasing surjective functions from  $[0, 1]$  to  $[0, 1]$ .

Let  $X$  be a set. A set  $\mathcal{R}$  where any  $r \in \mathcal{R}$  is of the form  $r \subseteq X$  is called a *set system* with *ground set*  $X$ . A pair  $(X, \mathcal{R})$  of a set system  $\mathcal{R}$  and its ground set  $X$  is called a SETCOVER instance. An optimal solution to a SETCOVER instance  $(X, \mathcal{R})$  is a set  $S^* \subset \mathcal{R}$  of minimal size, such that  $\bigcup_{s \in S^*} s = X$ .

**1.2 Problem definition** Let a polygonal curve  $P$  in  $\mathbb{R}^d$  and a radius  $\Delta > 0$  together with  $l \in \mathbb{N}$  be given. Following Akitaya et al. [5], for any curve  $C$  in  $\mathbb{R}^d$  we define

$$\text{Cov}_P(C, \Delta) = \left( \bigcup_{0 \leq s \leq t \leq 1, d_{\mathcal{F}}(P[s, t], C) \leq \Delta} [s, t] \right) \subset [0, 1]$$

as the  $\Delta$ -*coverage* of  $C$ , refer to Figure 1. The objective is to find the smallest (w.r.t. its cardinality) set  $\mathcal{C}$  of curves, each of complexity at most  $l$ , such that

$$\bigcup_{C \in \mathcal{C}} \text{Cov}_P(C, \Delta) = [0, 1].$$

This can be interpreted as computing the optimal solution of the SETCOVER instance

$$([0, 1], \{\text{Cov}_P(C, \Delta) \mid C \in \mathbb{X}_l^d\}).$$

This point of view is the main perspective, from which we will analyze this problem.

**1.3 Related work** The first work to appear in the line of clustering subtrajectories under both the discrete and continuous Fréchet distance was done by Buchin et al. [8], in which they analyze the problem of identifying a single cluster with certain properties which include the number of distinct subtrajectories or the length of the longest subtrajectory assigned to this cluster. They show hardness-results for  $(2 - \varepsilon)$ -approximations as well as a matching polynomial 2-approximation algorithm. Gudmundsson and Wong [14] then presented a cubic

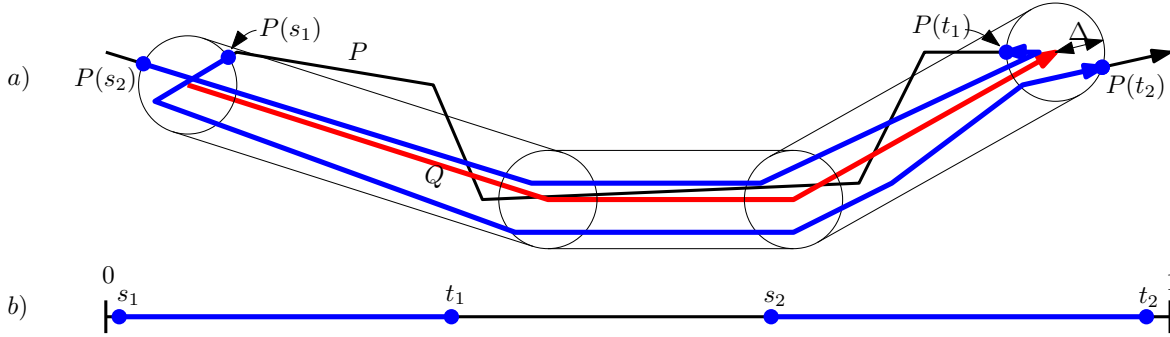


Figure 1: a): Example of all points on  $P$  that lie on subtrajectories of  $P$  that have Fréchet distance at most  $\Delta$  to a curve  $Q$  of complexity 3. b): The induced set  $\text{Cov}_P(Q, \Delta)$  as a subset of the parameter space of  $P$ , the unit interval  $[0, 1]$ .

lower-bound for this problem and show that this lower bound is tight. Gudmundsson and Valladares [13] investigated this approach further, presenting a practical implementation on a GPU. This approach was later on also used for road network reconstruction from GPS data [6, 7]. This approach was used similarly by Buchin, Kilgus and Kölzsch [9] to extract migration patterns from GPS data of migrating animals by repeatedly finding the largest cluster in the data and removing it, similar to the greedy SETCOVER algorithm.

None of these clustering approaches however offer theoretical guarantees as no explicit objective function for a cluster is formulated. One approach to define an objective function for a subtrajectory clustering problem is that of Agarwal et al. [1], in which they formulate an objective function similar to a facility location problem. That is they consider a weighted sum of qualities like the number of clusters, the radius of the clusters and the fraction of the curve that is not covered. For this problem they show conditional NP-hardness results but also give a  $O(\log^2 n)$ -approximation in case of certain well-behaved classes of curves under the discrete Fréchet distance.

The objective function for the subtrajectory clustering problem which we want to analyze further in this paper was introduced by Akitaya et al. [5]. They present a pseudo-polynomial bi-criterial approximation. That is they consider the problem from Section 1.2 and for given polygonal curve  $P$  of complexity  $n$ , complexity parameter  $l$  and radius  $\Delta$  they find a set of curves  $\mathcal{C}$  such that  $\bigcup_{C \in \mathcal{C}} \text{Cov}_P(C, \alpha\Delta) = [0, 1]$  of size  $O(l^2 \log(kl)k)$ . Here  $k$  is the smallest possible size of a set  $\mathcal{C}^*$ , whose coverage is  $[0, 1]$  and  $\alpha = O(1)$ . This was subsequently improved upon by Brüning et al. [4] to a polynomial algorithm with an expected running time of  $\tilde{O}(k^2n + kn^3)$  and slightly better approximation bounds. Their approach is based on computing a sufficiently small SET-

COVER instance with constant VC-dimension, which allows them to apply probabilistic  $\varepsilon$ -net finder algorithms with approximation guarantees in the VC-dimension. The constant VC-dimension comes at the cost of only considering center trajectories of complexity  $l = 1$ , sacrificing the quality of approximation.

**1.4 Our contribution** We present a new SETCOVER instance motivated by the works of Brüning et al. [4] which instead considers centers of non-constant complexity. This comes at the expense of the running time as well as the approximation guarantee but allows the identified clusters to be of higher significance especially under practical considerations. For a given polygonal curve of complexity  $n$  together with the parameter  $l$  and radius  $\Delta$  this new set system has size  $O(ln^3)$  instead of  $O(n^3)$ . Each set in this set system can consist of up to  $O(n)$  disjoint intervals in  $[0, 1]$ . As we store these explicitly the space requirement is  $O(ln^4)$ . The running time to construct this set system is  $O(l^2n^4)$ . It further takes  $O(kln^4 \log(n))$  time to then greedily and deterministically find a SETCOVER solution in this set system. We observe however, that in practice this dependency is significantly better, and evaluate our approach on GPS data of ocean drifters, with a total complexity of  $n \geq 10^6$ . We further evaluate our approach on high-dimensional full-body motion capture data and compare the output to a state-of-the-art motion segmentation algorithm to motivate that this approach has merit.

**1.5 Technical Overview** In Section 2 we revisit the results of Brüning et al. [4] redefining their notion of simplification which allows us to only consider subcurves of this simplification as possible centers of clusters. In Section 3 we extend their results to yield our new set system. We analyze its theoretical SETCOVER guarantees in Section 3.2. In Section 4 we discuss

some heuristical improvements we employed to improve the practical quality of the implementation. Finally in Section 5 we present an implementation of our approach and apply it to different data sets of very different types of motion tracking data and qualitatively evaluate its practicability.

## 2 A more structured set system

In this section we introduce the key players to our story. These allow us to impose some structure on the aforementioned set system at the cost of a constant approximation factor in both the radius, as well as the optimal solution size. With this reduction we follow Brüning et al. [4]. They combine the simplification of de Berg et al. [11] and Driemel et al. [12] retaining the central properties of both. It is defined as follows.

**DEFINITION 2.1. ( $\Delta$ -GOOD SIMPLIFICATION [4])** Let  $P$  be a polygonal curve in  $\mathbb{R}^d$  defined by the vertices  $(v_0, \dots, v_n)$  together with a parameter  $\Delta > 0$  be given. We call a curve  $S$  defined by the vertices  $(v_{i_0}, \dots, v_{i_k})$  for  $0 \leq i_0 < \dots < i_k \leq n$  a simplification of  $P$ . Denote the polygonal curve defined by the vertices  $(v_i, \dots, v_j)$  for some  $0 \leq i \leq j \leq n$  by  $P_{i,j}$ . We say a simplification defined by the vertices  $(v_{i_0}, \dots, v_{i_k})$  is  $\Delta$ -good if the following properties hold:

- (i)  $\|v_{i_j} - v_{i_{j+1}}\| \geq \frac{\Delta}{3}$  for  $0 \leq j < k$ ,
- (ii)  $d_{\mathcal{F}}(P_{i_j, i_{j+1}}, \overline{v_{i_j} v_{i_{j+1}}}) \leq 3\Delta$  for all  $0 \leq j < k$ ,
- (iii)  $d_{\mathcal{F}}(P_{1, i_1}, \overline{v_{i_1} v_{i_1}}) \leq 3\Delta$ ,
- (iv)  $d_{\mathcal{F}}(P_{i_k, n}, \overline{v_{i_k} v_{i_k}}) \leq 3\Delta$ ,
- (v)  $d_{\mathcal{F}}(P_{i_j, i_{j+2}}, \overline{v_{i_j} v_{i_{j+2}}}) > 2\Delta$  for all  $0 \leq j < k - 1$ .

These properties guarantee, that no edge is too short ((i)), the Fréchet distance of a  $\Delta$ -good simplification to its underlying curve is at most  $3\Delta$  ((ii) - (iv)) and that the complexity of a  $\Delta$ -good simplification can not greedily be reduced ((v)).

**LEMMA 2.1. ([4])** There is an algorithm that computes a  $\Delta$ -good simplification of any polygonal curve  $P$  in  $\mathbb{R}^d$  of complexity  $n$  and  $\Delta > 0$ . Furthermore it does so in  $O(n \log^2 n)$  time assuming  $d$  is a constant.

Brüning et al. [4] showed that any solution of the SETCOVER instance  $([0, 1], \{\text{Cov}_P(C, \Delta) \mid C \in \mathbb{X}_l^d\})$  induces a solution of the SETCOVER instance with set system  $\{\text{Cov}_P(S[s, t], 11\Delta) \mid 0 \leq s \leq t \leq 1, |S[s, t]| \leq l\}$  where  $S$  is some  $\Delta$ -good simplification of  $P$ .

**THEOREM 2.1. ([4])** Let a polygonal curve  $P$  and values  $\Delta > 0$  and  $l$  be given. Let  $S$  be a  $\Delta$ -good simplification of  $P$ . Let  $\mathcal{C}$  be a set of curves of size  $k$  each with complexity at most  $l$  such that  $\bigcup_{C \in \mathcal{C}} \text{Cov}_P(C, \Delta) = [0, 1]$ . Then there is a set  $\mathcal{C}_S$  of

size  $3k$  of subcurves of  $S$  each of which has complexity at most  $l$  with  $\bigcup_{C \in \mathcal{C}_S} \text{Cov}_S(C, 8\Delta) = [0, 1]$  and thus  $\bigcup_{C \in \mathcal{C}_S} \text{Cov}_P(C, 11\Delta) = [0, 1]$ .

## 3 A finite set-system

Similar to Brüning et al. [4] we now use the set system  $\{\text{Cov}_P(S[s, t], 11\Delta) \mid 0 \leq s \leq t \leq 1, |S[s, t]| \leq l\}$  as an intermediary set system. Based on this intermediary set system we introduce a new set system, which consists of only  $O(n^3 l)$  many subcurves of some  $\Delta$ -good simplification  $S$  of  $P$ .

### 3.1 Extremal Candidates

**DEFINITION 3.1. ( $\Delta$ -FREE SPACE)** Let  $P$  and  $Q$  be two polygonal curves parametrized over  $[0, 1]$ . The free space diagram of  $P$  and  $Q$  is their joint parameter space  $[0, 1]^2$  together with a not necessarily uniform grid, where each vertical line corresponds to a vertex of  $P$  and each horizontal line to a vertex of  $Q$ . The  $\Delta$ -free space of  $P$  and  $Q$  is defined as

$$\mathcal{D}_{\Delta}(P, Q) = \{(x, y) \in [0, 1]^2 \mid \|P(x) - Q(y)\| \leq \Delta\}$$

This is the set of points in the parametric space, whose corresponding points on  $P$  and  $Q$  are at a distance at most  $\Delta$ . The edges of  $P$  and  $Q$  segment the free space into cells. We call the intersection of  $\mathcal{D}_{\Delta}(P, Q)$  with the boundary of cells the  $\Delta$ -free space intervals. Refer to Figure 2 a).

Alt and Godau [2] showed that the  $\Delta$ -free space inside any cell is an ellipse intersected with the cell and thus convex and of constant complexity. They further showed that the Fréchet distance between two curves  $P$  and  $Q$  is less than or equal to  $\Delta$  if and only if there exists a path  $\pi : [0, 1] \rightarrow \mathcal{D}_{\Delta}(P, Q)$  that starts at  $(0, 0)$ , ends in  $(1, 1)$  and is monotone in both coordinates. By this analysis, two free subcurves  $P[a, c]$  and  $Q[b, d]$  have Fréchet distance at most  $\Delta$  if and only if there exists a path  $\pi : [0, 1] \rightarrow \mathcal{D}_{\Delta}(P, Q)$  that starts at  $(a, b)$ , ends in  $(c, d)$  and is monotone in both coordinates. Note that in the case of two free subcurves,  $\pi$  can be monotonically increasing or monotonically decreasing in its coordinates, depending only on if  $a \leq c$  or  $c \leq a$  and similarly  $b \leq d$  or  $d \leq b$ .

In order to reduce the size of the given set system for some polygonal curve  $P$  and  $\Delta$ , we inspect the  $11\Delta$ -free space of a  $\Delta$ -good simplification  $S$  of  $P$  with  $P$ . Conceptually, we want to do the following: Start with a subcurve  $S[s, t]$  of  $S$  that induces the set  $\text{Cov}_P(S[s, t], 11\Delta)$  in the set system.  $\text{Cov}_P(S[s, t], 11\Delta)$  can by definition be described as the union of intervals  $[a_i, b_i]$ , such that  $d_{\mathcal{F}}(S[s, t], P[a_i, b_i]) \leq 11\Delta$ . Now the

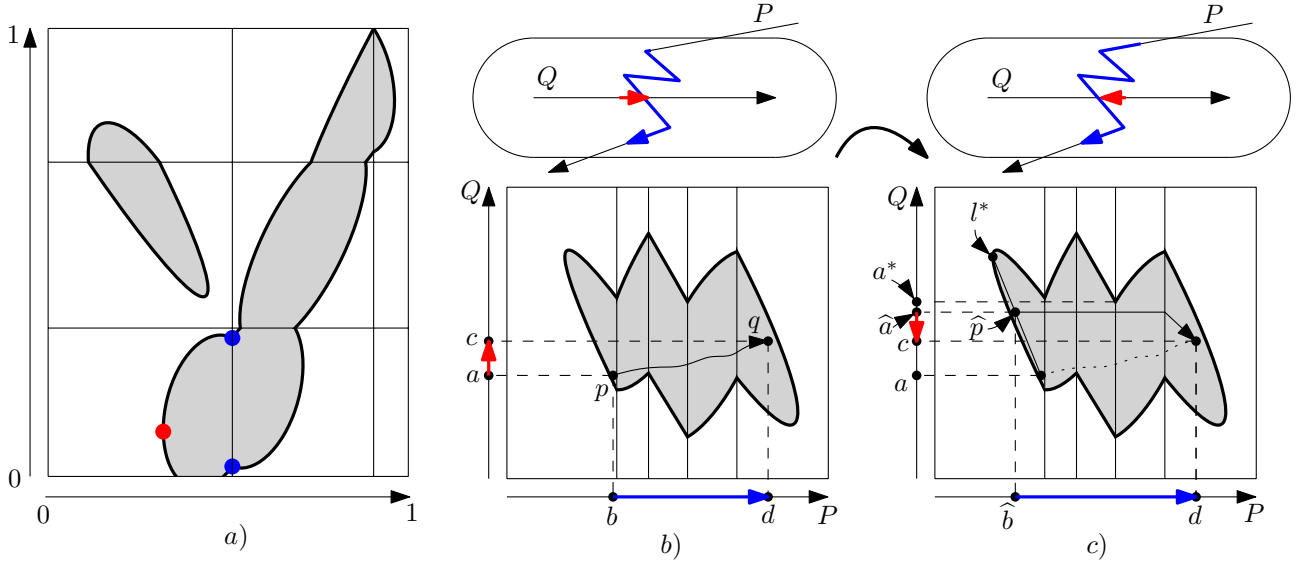


Figure 2: a): Example of the  $\Delta$ -free space of two curves. Further illustrated is the unique left  $\Delta$ -extremal point in red in the free space as well as the two right  $\Delta$ -extremal points in blue in the lower left cell of the  $\Delta$ -free space. b), c): Illustration to the proof of Lemma 3.1. Depicted are the  $\Delta$ -free spaces of  $P$  and  $Q$ , as well as the path from  $p$  to  $q$  before the modification in b) and from  $\hat{p}$  to  $q$  after the modification in c) as in the proof of Lemma 3.1.

point  $(a_i, s)$  lies in some cell, and this cell has a (not necessarily unique) left-most point. We would like to modify  $s$  and  $t$  as well as all  $a_i$  and  $b_i$  in such a way, that (i) the new values  $s'$  and  $t'$  of  $s$  and  $t$  are defined by the  $y$ -coordinates of a left-/right-most point in some cell of the  $11\Delta$ -free space and (ii) the resulting interval  $[a'_i, b'_i]$  includes  $[a_i, b_i]$ . While this is not necessarily possible, we prove that this can be achieved with a constant number of such subcurves of  $S$ .

**DEFINITION 3.2. ( $\Delta$ -EXTREMAL POINTS)** Let  $P$  and  $Q$  be two polygonal curves parametrized over  $[0, 1]$ . For every cell  $C$  of the free space diagram of  $P$  and  $Q$  define its left  $\Delta$ -extremal points as either the unique left-most point inside the  $\Delta$ -free space in  $C$  or, in case the left-most point is not unique, the upper-most and lower-most left-most point inside the  $\Delta$ -free space in  $C$ . Similarly define the right  $\Delta$ -extremal points of each  $C$ . The union of left (resp. right)  $\Delta$ -extremal points of all cells is defined to be the set of left (resp. right)  $\Delta$ -extremal points of  $P$  and  $Q$ . Refer to Figure 2 a).

Observe that for given polygonal curves  $P$  and  $Q$  of complexity  $n$  the set of  $\Delta$ -extremal points can be computed in  $O(n^2)$  time by scanning over every cell and computing these points in  $O(1)$ .

**LEMMA 3.1.** Let two subcurves  $P[a, c]$  and  $Q[b, d]$  of polygonal curves  $P$  and  $Q$  as well as a value  $\Delta > 0$  be given such that  $d_{\mathcal{F}}(P[a, c], Q[b, d]) \leq \Delta$ . Then there

are values  $b^*, d^* \in [0, 1]$  defined by  $y$ -coordinates of  $\Delta$ -extremal points of  $P$  and  $Q$  such that for any  $\hat{b}$  between  $b$  and  $b^*$  and any  $\hat{d}$  between  $d$  and  $d^*$  the free subcurve  $Q[\hat{b}, \hat{d}]$  of  $Q$  induces a subcurve  $P[\hat{a}, \hat{c}]$  of  $P$  with  $d_{\mathcal{F}}(P[\hat{a}, \hat{c}], Q[\hat{b}, \hat{d}]) \leq \Delta$  and  $[a, c] \subset [\hat{a}, \hat{c}]$ .

*Proof.* Since  $d_{\mathcal{F}}(P[a, c], Q[b, d]) \leq \Delta$ , there is a path  $\pi : [0, 1] \rightarrow \mathcal{D}_{\Delta}(P, Q)$  that starts at  $p = (a, b)$ , ends in  $q = (c, d)$  and is monotone in both coordinates. First check if the left  $\Delta$ -extremal point  $l^*$  of the cell containing  $p$  is above or below the point  $p$ . In case of ambiguity pick either one of the two left  $\Delta$ -extremal points of the cell containing  $p$  to be  $l^*$ . If  $l^*$  lies above  $p$ , define  $b^*$  as the  $y$ -coordinate of the lowest left  $\Delta$ -extremal point in the  $\Delta$ -free space of  $P$  and  $Q$  that is above  $p$ . Otherwise define  $b^*$  as the  $y$ -coordinate of the highest left  $\Delta$ -extremal point that is below  $p$ . Now let  $\hat{b}$  be given as a value inbetween  $b$  and  $b^*$ . As  $\hat{b}$  lies in between the  $y$ -coordinate of  $p$  and that of  $l^*$ , there is a point  $\hat{p}$  on the line from  $p$  to  $l^*$  with  $y$ -coordinate  $\hat{b}$ . Observe that  $\hat{p}$  always lies to the left of  $p$ . Thus for the  $x$ -coordinate  $\hat{a}$  of  $\hat{p}$  we have that  $[a, c] \subset [\hat{a}, \hat{c}]$ .

We now show that there is a monotone path from  $\hat{p}$  to  $q$  inside the  $\Delta$ -free space and thus  $d_{\mathcal{F}}(P[\hat{a}, \hat{c}], Q[\hat{b}, \hat{d}]) \leq \Delta$ . Assume that  $\hat{p}$  lies above  $p$ , as otherwise by convexity of the free space in every cell we can concatenate a straight line from  $\hat{p}$  to  $p$  with  $\pi$ .

First, observe that we can walk straight to the right from  $\hat{p}$  until we either intersect the path  $\pi$  or intersect

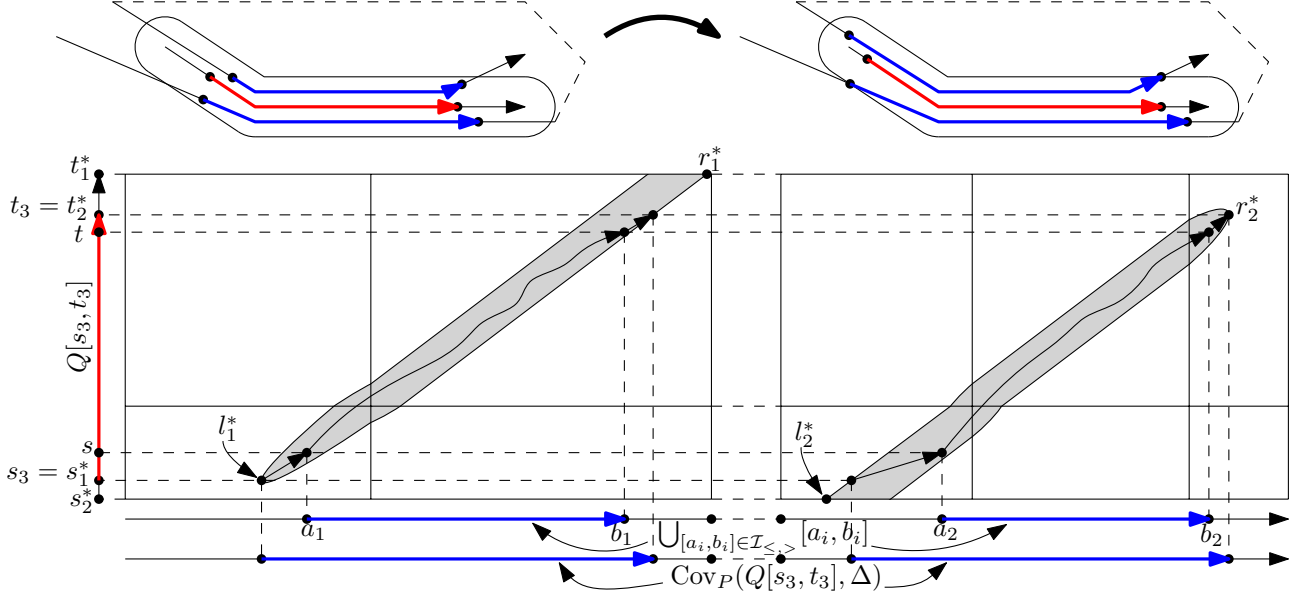


Figure 3: Illustration for the proof of Theorem 3.1. The inclusion-wise increase of the  $\Delta$ -Coverage for all intervals in  $\mathcal{I}_{<, >} = \{[a_1, b_1], [a_2, b_2]\}$  is depicted. The intervals  $[a_1, b_1]$  and  $[a_2, b_2]$  are in  $\mathcal{I}_{<, >}$  because the left  $\Delta$ -extremal points  $l_1^*$  and  $l_2^*$  of the cells containing  $(a_1, s)$  and  $(a_2, s)$  lie below  $s$ , and similarly  $r_1^*$  and  $r_2^*$  lie above  $t$ .

the boundary of the cell containing  $q$  on the right side. Indeed, every free space interval that contains the  $y$ -coordinate of  $p$  also contains the  $y$ -coordinate of  $\hat{p}$  by definition of  $b^*$ . If the ray intersects  $\pi$  then, again, we can construct such a path by concatenating a straight line from  $\hat{p}$  to this intersection point with the second piece of  $\pi$ . Hence, assume the straight line does not intersect  $\pi$  until it intersects the boundary of the cell containing  $q$ . Then, we construct the path by walking from  $\hat{p}$  to the right, until we first enter the cell containing  $q$  and then by convexity we can again connect this straight line with a second straight line to  $q$  resulting in a monotone path.

Next we construct  $d^*$  in a similar fashion, except we use the right-most point  $r^*$  of the cell containing  $q$  instead of left-most points. Yielding both  $b^*$  and  $d^*$  together with a path from  $\hat{p}$  to  $\hat{q}$  for any  $\hat{b}$  in between  $b$  and  $b^*$  and  $\hat{d}$  in between  $d$  and  $d^*$ .  $\square$

**THEOREM 3.1.** *Let  $P$  and  $Q$  be two given polygonal curves together with a value  $\Delta > 0$ . For every  $s, t \in [0, 1]$  there are at most eight values  $s_1, \dots, s_4, t_1, \dots, t_4 \in [0, 1]$  defined by  $y$ -coordinates of  $\Delta$ -extremal points of  $P$  and  $Q$  such that*

$$\text{Cov}_P(Q[s, t], \Delta) \subset \bigcup_{i=1}^4 \text{Cov}_P(Q[s_i, t_i], \Delta).$$

*Proof.* An illustration to this proof can be seen in Figure 3. Let  $\mathcal{I} = \{[a_i, b_i] \subset [0, 1] \mid d_{\mathcal{F}}(P[a_i, b_i], Q[s, t]) \leq$

$\Delta\}$  be the set of intervals defining  $\text{Cov}_P(Q[s, t], \Delta)$ . Partition  $\mathcal{I}$  into four sets, according to whether for  $[a_i, b_i]$  the values  $s_i^*$  and  $t_i^*$  from Lemma 3.1 is above or below  $s$  and above or below  $t$ . That is

$$\begin{aligned} \mathcal{I}_{\leq, \leq} &= \{[a_i, b_i] \in \mathcal{I} \mid s_i^* \leq s, t_i^* \leq t\} \\ \mathcal{I}_{>, \leq} &= \{[a_i, b_i] \in \mathcal{I} \mid s_i^* > s, t_i^* \leq t\} \\ \mathcal{I}_{\leq, >} &= \{[a_i, b_i] \in \mathcal{I} \mid s_i^* \leq s, t_i^* > t\} \\ \mathcal{I}_{>, >} &= \{[a_i, b_i] \in \mathcal{I} \mid s_i^* > s, t_i^* > t\}. \end{aligned}$$

Now for  $\mathcal{I}_{\leq, \leq}$  observe that the set of  $s_i^*$  as well as the set of  $t_i^*$  is finite, as there can be at most  $O(n^2)$  many distinct left or right  $\Delta$ -extremal points. Thus

$$\begin{aligned} s_1 &= \max\{s_i^* \mid [a_i, b_i] \in \mathcal{I}_{\leq, \leq}\}, \\ t_1 &= \max\{t_i^* \mid [a_i, b_i] \in \mathcal{I}_{\leq, \leq}\} \end{aligned}$$

are well defined, and  $s_1$  lies between  $s$  and any  $s_i^*$  in  $\{s_i^* \mid [a_i, b_i] \in \mathcal{I}_{\leq, \leq}\}$  and  $t_1$  lies between  $t$  and any  $t_i^*$  in  $\{t_i^* \mid [a_i, b_i] \in \mathcal{I}_{\leq, \leq}\}$ . Thus by Lemma 3.1 There are values  $\hat{a}_i$  and  $\hat{b}_i$  for every  $[a_i, b_i] \in \mathcal{I}_{\leq, \leq}$ , such that  $d_{\mathcal{F}}(P[\hat{a}_i, \hat{b}_i], Q[s_1, t_1]) \leq \Delta$ , and thus

$$\bigcup_{[a_i, b_i] \in \mathcal{I}_{\leq, \leq}} [a_i, b_i] \subset \text{Cov}_Q(P[s_1, t_1], \Delta).$$

Similarly we can identify

$$\begin{aligned} s_2 &= \min\{s_i^* \mid [a_i, b_i] \in \mathcal{I}_{>, \leq}\}, \\ t_2 &= \max\{t_i^* \mid [a_i, b_i] \in \mathcal{I}_{>, \leq}\}, \\ s_3 &= \max\{s_i^* \mid [a_i, b_i] \in \mathcal{I}_{\leq, >}\}, \end{aligned}$$

$$\begin{aligned}
t_3 &= \min\{t_i^* \mid [a_i, b_i] \in \mathcal{I}_{\leq, >}\}, \\
s_4 &= \min\{s_i^* \mid [a_i, b_i] \in \mathcal{I}_{>, >}\}, \\
t_4 &= \min\{t_i^* \mid [a_i, b_i] \in \mathcal{I}_{>, >}\}.
\end{aligned}$$

As  $\mathcal{I}_{\leq, \leq}, \mathcal{I}_{>, \leq}, \mathcal{I}_{\leq, >}$  and  $\mathcal{I}_{>, >}$  partition  $\mathcal{I}$ , it follows that

$$\begin{aligned}
\text{Cov}_P(Q[s, t], \Delta) &= \bigcup_{[a_i, b_i] \in \mathcal{I}} [a_i, b_i] \\
&\subset \bigcup_{i=1}^4 \text{Cov}_P(Q[s_i, t_i], \Delta),
\end{aligned}$$

proving the claim.  $\square$

**THEOREM 3.2.** *Let a polygonal curve  $P$  in  $\mathbb{R}^d$  of complexity  $n$  and values  $\Delta > 0$  and  $l \in \mathbb{N}$  be given. A set of curves  $\mathcal{S} \subset \mathbb{X}_l^d$  of size  $O(n^3 l)$  can be computed in time  $O(n^3 l^2)$  with the following property. If there is a set  $\mathcal{C} \subset \mathbb{X}_l^d$  of size  $k$  such that  $\bigcup_{C \in \mathcal{C}} C = [0, 1]$ , then there is a set  $\mathcal{C}_S \subset \mathcal{S}$  of size  $12k$  with  $\bigcup_{C \in \mathcal{C}_S} C = [0, 1]$ .*

*Proof.* First compute a  $\Delta$ -good simplification  $S$  of  $P$  in time  $O(n \log^2 n)$ , which is possible by Lemma 2.1. Next compute the  $11\Delta$ -free space and subsequently the left and right  $11\Delta$ -extremal points of  $S$  and  $P$  in time  $O(n^2)$ . For every left  $11\Delta$ -extremal point  $s$  and every right  $11\Delta$ -extremal point  $t$  such that  $|S[s, t]| \leq l$  store  $S[s, t]$  in  $\mathcal{S}$ . This takes  $O(n^2) \cdot O(ln) \cdot O(l)$  time. The correctness of the property is an immediate consequence of Theorem 2.1 and Theorem 3.1.  $\square$

**3.2 Discretization of the ground set** So far we have presented a discretization of the set system to our original SETCOVER instance, which preserves the optimal solution up to a bounded approximation factor. This allows us to apply SETCOVER solving techniques such as a greedy algorithm [23], which chooses sets incrementally and in each step chooses the set which increases the accumulated coverage of the ground set the most. In the following, we argue that this can be done efficiently.

**LEMMA 3.2.** *Let  $P$  and  $Q$  be two polygonal curves of complexity at most  $n$  and a parameter  $\Delta > 0$  be given. Then  $\text{Cov}_P(Q, \Delta)$  can be written as the union of  $O(n)$  disjoint closed intervals.*

*Proof.* Let  $P[a, b]$  be a subcurve of  $P$ , such that  $d_{\mathcal{F}}(P[a, b], Q) \leq \Delta$ . Then,  $(a, 0)$  is contained in the  $\Delta$ -free space of some cell. Let  $(a^*, 0)$  be the leftmost point in the cell containing  $(a, 0)$ . We can concatenate  $\overline{a^*, a}$  to any monotone path starting in  $a$ . Thus, any path starting in the cell containing  $(a, 0)$  may as well start in  $(a^*, 0)$ . Similarly, any path may as well end in a

rightmost point  $(b^*, 1)$  of some cell. Thus,  $\text{Cov}_Q(P, \Delta)$  consists of a union of intervals, each interval starting and ending in one of at most  $n$  points.  $\square$

**THEOREM 3.3.** *Let  $P$  be a polygonal curve, and let  $\Delta > 0$  and  $l \in \mathbb{N}$  be given. There is an algorithm, computing a  $O(\log(n))$ -approximation for the SETCOVER instance  $([0, 1], \{\text{Cov}_P(S, 11\Delta) \mid S \in \mathcal{S}\})$ , where  $\mathcal{S}$  is as in Theorem 3.2.*

*Proof.* An immediate consequence of Lemma 3.2 is that the arrangement of all sets contained in some set of the set family consists of at most  $O(n^4 l)$  intervals  $\mathcal{I}$ . Interpreting these intervals as discrete objects, we now get a transformed SETCOVER instance

$$\left( \mathcal{I}, \left\{ \bigcup_{I \in \mathcal{I}, I \subset \text{Cov}_P(S, 11\Delta)} I \mid S \in \mathcal{S} \right\} \right).$$

Applying the greedy SETCOVER algorithm to this yields a  $O(\log(n^4 l)) = O(\log n)$  approximation algorithm in the size of an optimal solution.  $\square$

**COROLLARY 3.1.** *Let a polygonal curve  $P$  of complexity  $n$  and values  $\Delta > 0$  and  $l \in \mathbb{N}$  be given. There exists an algorithm that computes a set of curves  $\mathcal{C}$ , each of complexity at most  $l$  such that  $\bigcup_{C \in \mathcal{C}} \text{Cov}_P(C, 11\Delta) = [0, 1]$  in  $\tilde{O}(l^2 n^4 + k l n^4)$  time. Further  $|\mathcal{C}| \in O(\log(n)k)$ , where  $k$  is the smallest cardinality of any set  $\mathcal{C}^* \subset \mathbb{X}_l^d$  such that  $\bigcup_{C \in \mathcal{C}^*} \text{Cov}_P(C, 11\Delta)$ .*

*Proof.* It is left to show that for any subcurve  $C$  of  $S$  of complexity  $l$  we can compute  $\text{Cov}_P(C, 11\Delta)$  in  $O(ln)$  time given the  $11\Delta$ -Freespace of  $\mathcal{S}$  and  $P$ . Further we need to show that for a given partial solution  $S^*$  of size  $O(\log(n)k)$  and a given subcurve  $C$  of  $\mathcal{S}$  we can compute the covered fraction from the intervals of the arrangement in  $\text{Cov}_P(C, 11\Delta) \setminus \bigcup_{S \in S^*} \text{Cov}_P(S, 11\Delta)$  to update  $C$  for the greedy SETCOVER algorithm in  $\tilde{O}(n)$ . The first part is straightforward, as the part of the  $11\Delta$ -Freespace we have to consider is of size  $O(ln)$ . We need to traverse it once from bottom left to top right to compute the  $11\Delta$ -Coverage of such a subcurve. For the second part, observe that  $k \leq n$ , as a possible solution consists of all the edges of  $P$ . Thus, as any  $11\Delta$ -coverage consists of at most  $O(n)$  intervals the  $11\Delta$ -Coverage of any partial solution consists of at most  $O(n^2)$  disjoint intervals, which we store in an interval-tree. Any interval in this interval-tree also stores the number of intervals of the arrangement that are not covered and lie to the left of its left boundary. With this information we can compute the number of intervals of the arrangement in  $\text{Cov}_P(C, 11\Delta) \setminus$

$\bigcup_{S \in S^*} \text{Cov}_P(S, 11\Delta)$  in  $O(n \log(n^2)) = O(n \log n)$  time. Updating the information in the interval-tree upon increasing the partial solution can be done in  $\tilde{O}(n^3)$  time and needs to be done at most  $O(k \log n)$  times.  $\square$

#### 4 Practical Improvements

In our implementation we use a modified set system. We do not use the full set of  $11\Delta$ -extremal points of the  $11\Delta$ -free space of the  $\Delta$ -good simplification  $S$  with itself, but only a sufficient subset, yielding the same theoretical guarantees. For this, we observe that if e.g. the left  $11\Delta$ -extremal points in some cell  $C$  lies on the left boundary of  $C$  (that is they coincide with the boundary of the left free-space interval of  $C$ ) we can extend any path starting in such an extremal point to start in the cell to the left of  $C$ . We further observe that any subcurve of the computed  $\Delta$ -good simplification for a given input resulting from Theorem 3.1 is never determined by the *lower* left  $11\Delta$ -extremal point, if the left  $11\Delta$ -extremal point is not unique, with the exception of the case where the left  $11\Delta$ -extremal point lies on the boundary of the entire free space diagram.

Together this results in the following modified set of  $11\Delta$ -extremal points, which we use to compute the candidate set of subcurves of  $S$  in the implementation: If a cell has a unique left  $11\Delta$ -extremal point, then we add this point to the set of relevant start points. If the left  $11\Delta$ -extremal point is not unique, then we draw a straight line from the upper left  $11\Delta$ -extremal point  $p$  to the left until the line intersects the boundary of  $11\Delta$ -free space in some cell  $C^*$ . Only if all left  $11\Delta$ -extremal points of  $C^*$  lie above this intersection point, we add the point  $p$  to the relevant start points. Otherwise we could extend any monotone path starting in  $p$  to start in any left  $11\Delta$ -extremal point of  $C^*$ , which we also consider for the relevant start points. Lastly, we add all lower left  $\Delta$ -extremal points of cells on the left boundary of the free space diagram to the relevant start points, covering the described edge-case. We similarly identify the subset of relevant start points of free subcurves that are not subcurves of  $S$  (i.e. where the path of the matched subcurves is monotonically decreasing in the  $y$ -coordinate), as they are never determined by *upper* left  $11\Delta$ -extremal points. We similarly identify only the relevant endpoints and finally we combine these sets to obtain a sufficient set of free subcurves of  $S$ .

Computing these candidates can still be done in  $O(ln^3)$  time. Observe that the theoretical guarantees of the set system do not get better, as there may still be  $O(n^2)$  such relevant start points and end points. Further, we observe that we obtain the same theoretical guarantees on the approximation. The analysis is the

same as in the proof of Theorem 3.1, with the minor exception that in the analysis in Lemma 3.1 the path from  $s$  to  $s^*$  is no longer a straight line with  $s^*$  being the left  $11\Delta$ -extremal point of the cell containing  $s$ . Instead it is the path described above, in which we start in  $s$  and go to the left  $11\Delta$ -extremal point  $s^*$  of the cell  $C^*$  we ended up in, by going as far to the left (and only down resp. only up) as we could without leaving the row of cells containing  $s$ . And thus any starting  $y$ -coordinate  $\hat{s}$  that lies between the  $y$ -coordinates of  $s$  and  $s^*$  induces a subcurve of  $S$  whose covering is a superset of the subcurve starting in  $s$ . This analysis similarly extends to the endpoint and carries over to Theorem 3.1.

We make use of a further modification in which we define the size of the sets not by the number of intervals in the arrangement that are contained in the  $11\Delta$ -Coverage, but instead by the total length of the intervals represented by its  $11\Delta$ -Coverage. Conceptually we can think of this as discretizing the ground set  $[0, 1]$  via a regular grid with cell length  $\varepsilon > 0$ . This leads to an  $O(\log(\varepsilon^{-1}))$  approximation as the number of grid points inside an interval approximate the length of the intervals, and an additional additive error in the radius. The algorithm does not need to know  $\varepsilon$ .

#### 5 Experiments

We now analyze the practical running time and perform a qualitative evaluation of the computed clusterings in two application settings: (1) behavioral analysis and (2) Earth system analysis. In Section 5.3 we compare the output of the algorithm against a well-known motion segmentation algorithm on full-body motion data. In Section 5.4 we consider ocean drifter data and we evaluate the total complexity of the set system observing that the complexity is significantly lower than suggested by our upper bounds.

**5.1 Experimental Setup** All code was written in C++ and compiled with `clang` version 16.0.6 using the `-O3` optimization flag. The code is available [3]. All experiments were conducted on a MacBook Air with 8GB of RAM and a Apple M1 processor.

**5.2 Data sets** We run our experiments on two different data sets. The first is the well-established CMU data set [21]. Here we apply our algorithm to each trial of subject 86 and compare the resulting segmentation to the segmentation of Zhou et al. [28]. The second data set is a subset of the quality-controlled 6-hour interpolated data from ocean surface drifting buoys [19] consisting of roughly 2000 trajectories, where each consists of up to 1000 vertices on a sphere, i.e. three dimensions.

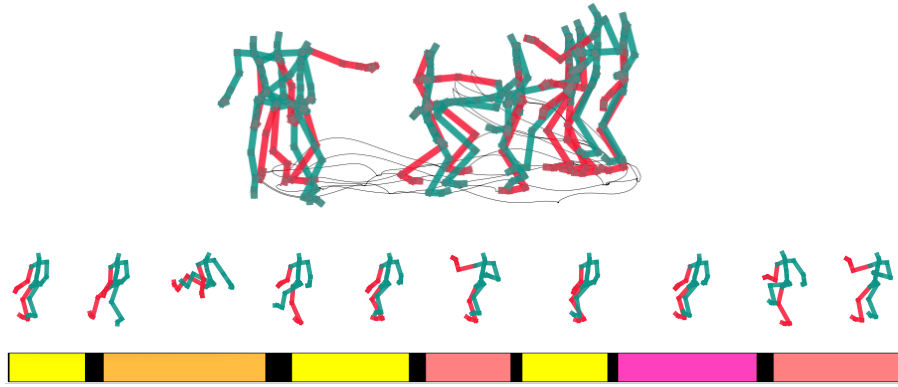


Figure 4: Illustration of CMU subject 86 trial 01 and the ground truth labels from [16] along the time axis. Yellow corresponds to the label *walk*, orange to *jump*, light red to *punch* and magenta to *kick*, while black corresponds to transitions between labels.

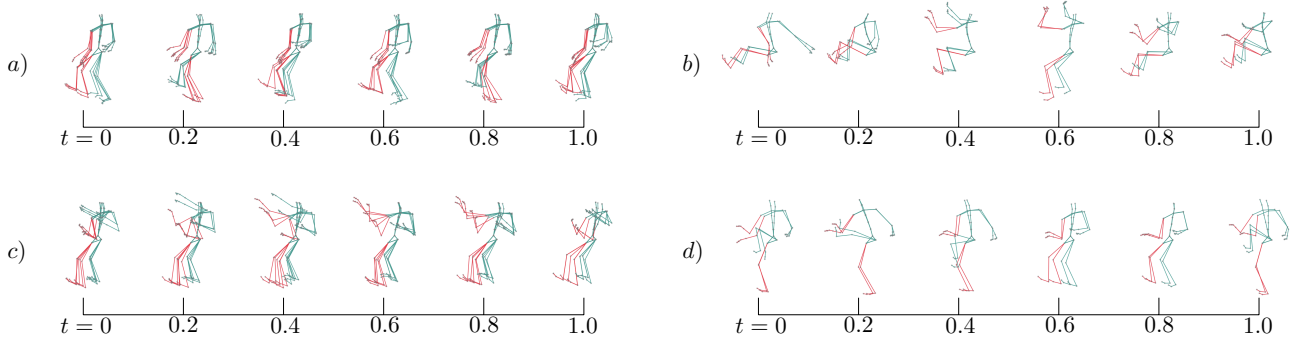


Figure 5: Illustration of the subcurves computed by our algorithm corresponding to the coverage of the first four clusters of the curve CMU 86 trial 01 found during the greedy SETCOVER algorithm (with  $\Delta = 1.25$  and  $l = 10$ ) corresponding to the four labeled actions *a)* *walk*, *b)* *jump*, *c)* *punch* and *d)* *kick*.

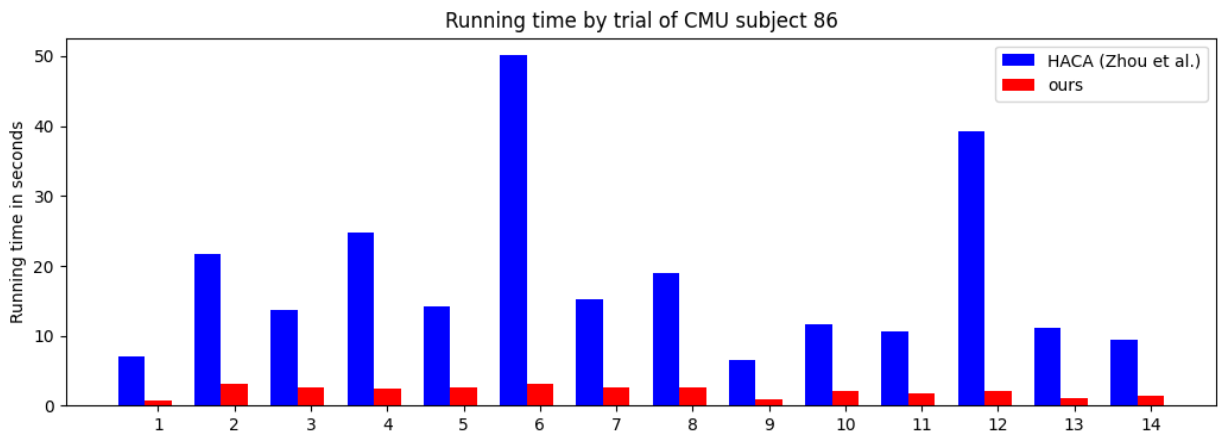


Figure 6: Running time of HACA [28] and our implementation on the 14 trials of CMU subject 86.

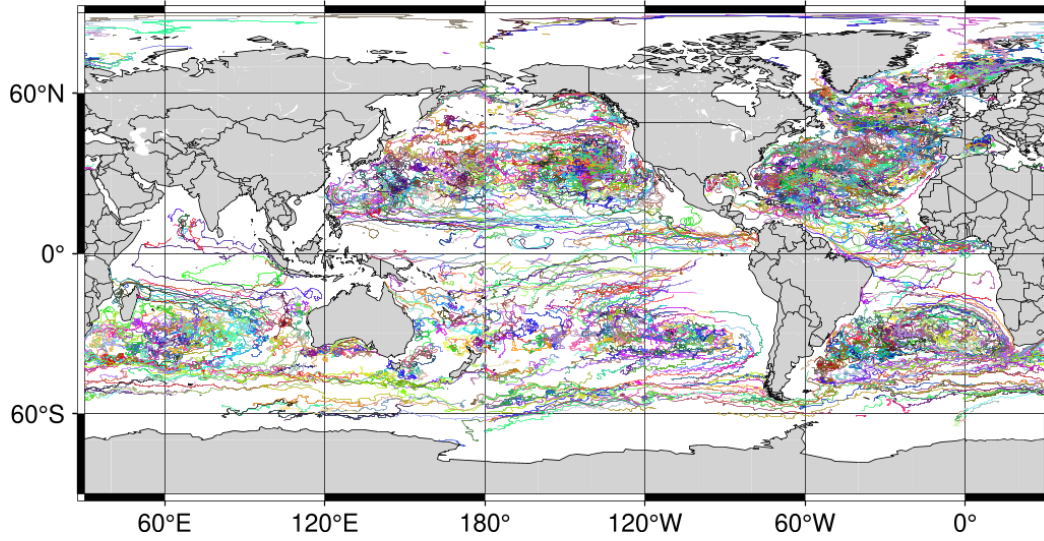


Figure 7: Surface Drifter Data set of data recorded between the years of 2022 and 2023 (2108 different drifters). Different colors correspond to different surface drifters.

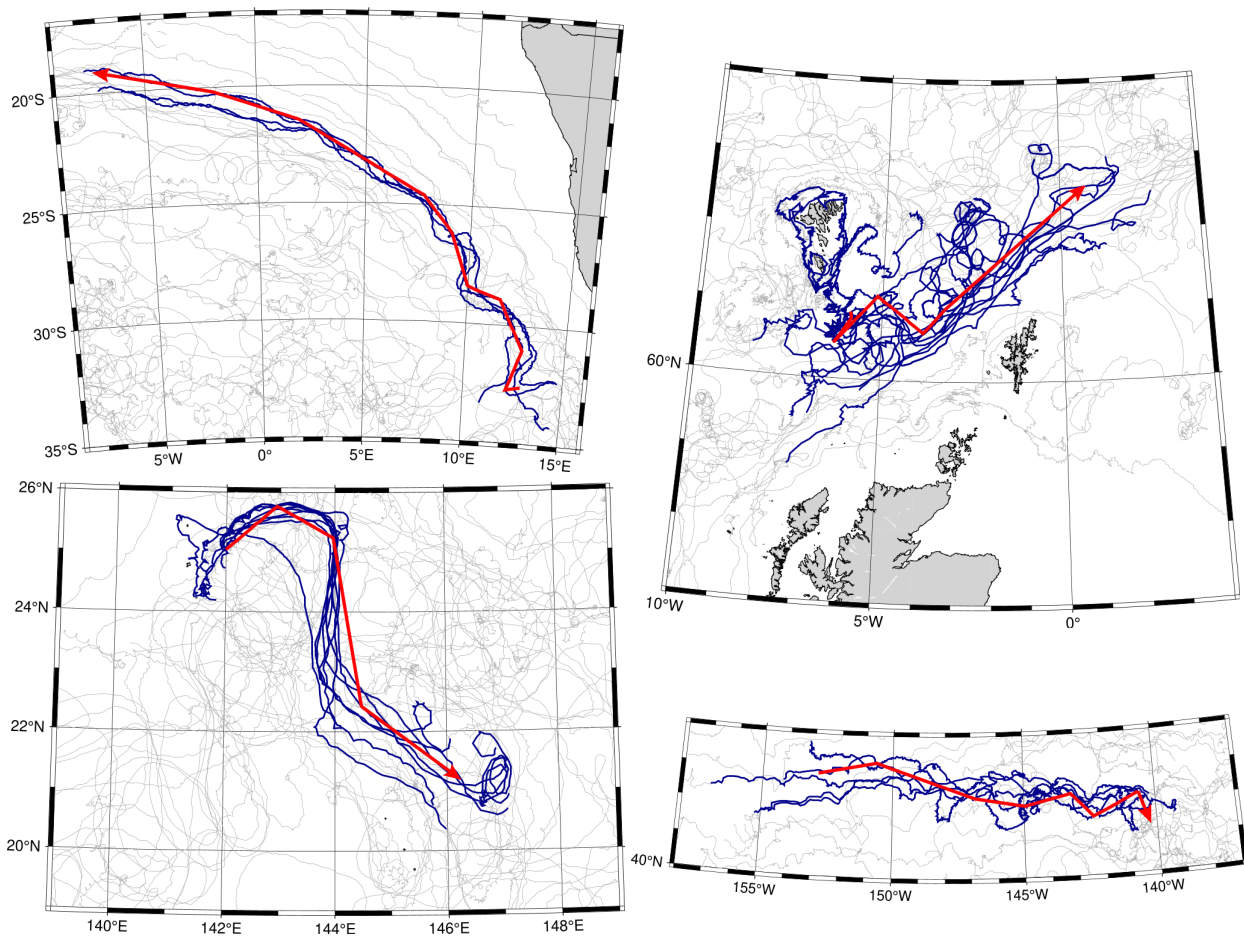


Figure 8: Four curves (red) and their approximate coverage (blue) selected during the first 10 greedy SETCOVER selections on the Global Drifter Program Data with  $\Delta = 15\text{km}$  and  $l = 10$ .

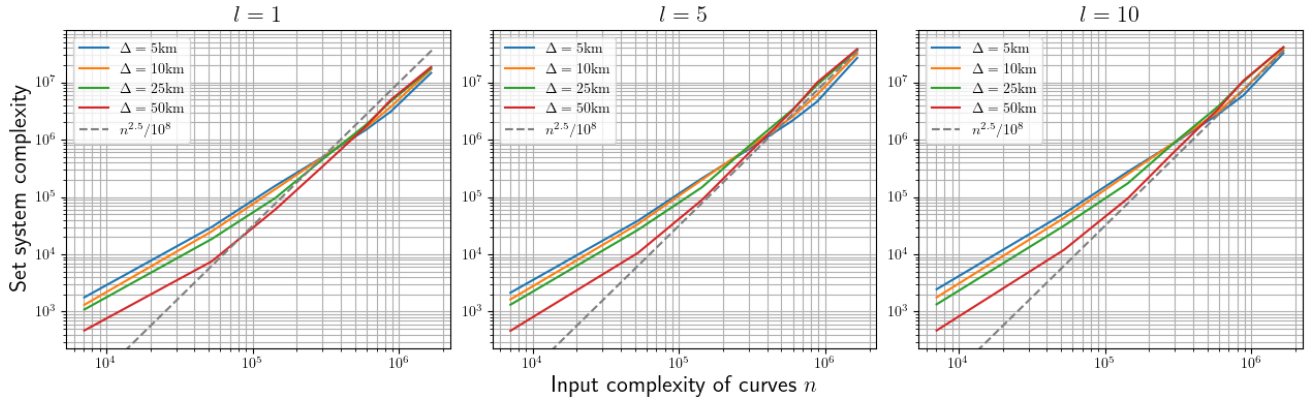


Figure 9: Set system complexity vs. input complexity for different values of  $\Delta$  and  $l$ .

**5.3 CMU Motion Capture Data** Motion Segmentation is a long standing problem that finds applications in many different fields such as robotics, sports analysis or traffic monitoring [20]. We apply our techniques to this problem on the CMU data set [21]. This data set consists of motion tracking data of 31 different joint-trackers on different subjects doing sports (trials) ranging through different activities (refer to Figure 4). We interpret these as trajectories in 93-dimensional Euclidean space by concatenating the three-dimensional coordinates of all joints back to back. Each trial consists of up to  $10^4$  vertices. We compare the resulting segmentations to ground truth data from [16] and the hierarchical aligned cluster algorithm proposed by Zhou et al. [28]. We then apply our subtrajectory clustering algorithm with a radius of  $\Delta = 1.25$  and a complexity bound of  $l = 10$ . The output then consists of a set of curves that act as cluster centers. For each of these centers we identify the ground truth label that corresponds the best to this center and label all points in its  $11\Delta$ -Coverage with the identified label. Whenever multiple different labels are assigned to a point along the curve we mark it as a transition between different motions. The resulting labeling can be seen in Figure 10 in the appendix. The subtrajectories that correspond to the coverage of the largest clusters found during the greedy SETCOVER algorithm can be seen in Figure 5. A comparison in running time can be seen in Figure 6.

**5.4 Global Drifter Program** A different application where vast amounts of trajectory data is analyzed to identify underlying patterns is found in the analysis of oceanic processes [25]. One goal is the estimation of static currents on the surface of the ocean. A comprehensive and often used data set in this area is that of the NOAA Global Drifter Program [19], which consists of almost 20000 surface drifters that have been released

across the ocean as far back as 1979. For our evaluation we focus on the subset of trajectories consisting of all drifters recorded in the last year (2022 - 2023), refer to Figure 7. These consist of 2108 different trajectories which consist on average of 500 points resulting in a total input complexity of  $n \geq 10^6$ . We apply our techniques with a radius of  $\Delta = 15\text{km}$  and a complexity bound of  $l = 10$  to identify subtrajectory clusters in these drifter trajectories. Figure 8 shows a selection of four clusters from the first 14 cluster centers chosen by the greedy set cover algorithm together with their corresponding  $11\Delta$ -Coverage. The first 14 clusters computed via greedy set cover are included in the appendix (Figure 11 and Figure 12). Figure 13 shows the first 500 cluster centers.

Despite an asymptotic running time of  $\tilde{O}((k+l)ln^4)$  our techniques can still be applied here. This is likely due to the property that the curves are spatially spread out and many pairs of subcurves are never considered to be in the same cluster. Figure 9 shows the total number of intervals in the set system for different  $l$  and  $\Delta$ , which is in  $O(ln^4)$  but compares favorably with  $10^{-8}n^{2.5}$ .

## 6 Conclusions

In this paper we extended the works of Akitaya et al. [5] and Brüning et al. [4] to obtain a bi-criterial approximation algorithm for the subtrajectory clustering problem. We presented evidence that in practice the size and complexity of the set system generated by the algorithm on real data is considerably better than  $\tilde{O}(ln^4)$  as suggested by the theoretical analysis. We further show that the running time compares favorably to a state-of-the-art algorithm for full-body motion segmentation. We believe that our results demonstrate the practical viability of subtrajectory clustering algorithms with theoretical guarantees based on the Fréchet distance.

## Acknowledgements

We thank Frederik Brüning for contributions in early stages of this research. We thank Jürgen Gall, Julian Tanke, Jürgen Kusche, and Bernd Uebbing for useful discussions on the data sets and real world problems.

## References

- [1] Pankaj K. Agarwal, Kyle Fox, Kamesh Munagala, Abhinandan Nath, Jiangwei Pan, and Erin Taylor. Subtrajectory clustering: Models and algorithms. In *Proceedings of the 37th ACM SIGMOD-SIGACT-SIGAI Symposium on Principles of Database Systems*, PODS '18, page 75–87, 2018. doi:10.1145/3196959.3196972.
- [2] Helmut Alt and Michael Godau. Computing the Fréchet distance between two polygonal curves. *Int. J. Comput. Geom. Appl.*, 5:75–91, 1995. doi:10.1142/S0218195995000064.
- [3] Anonymous Author. Anonymous github repository. <https://anonymous.4open.science/r/clustering-0EEA/>, 2023.
- [4] Frederik Brüning, Jacobus Conradi, and Anne Driemel. Faster Approximate Covering of Subcurves Under the Fréchet Distance. In *30th Annual European Symposium on Algorithms (ESA 2022)*, volume 244 of *Leibniz International Proceedings in Informatics (LIPIcs)*, pages 28:1–28:16, Dagstuhl, Germany, 2022. Schloss Dagstuhl – Leibniz-Zentrum für Informatik. doi:10.4230/LIPIcs.ESA.2022.28.
- [5] Frederik Brüning, Hugo Akitaya, Erin Chambers, and Anne Driemel. Subtrajectory clustering: Finding set covers for set systems of subcurves. *Computing in Geometry and Topology*, 2(1):1:1–1:48, Feb. 2023. URL: <https://www.cgt-journal.org/index.php/cgt/article/view/7>, doi:10.57717/cgt.v2i1.7.
- [6] Kevin Buchin, Maike Buchin, David Duran, Britany Terese Fasy, Roel Jacobs, Vera Sacristan, Rodrigo I. Silveira, Frank Staals, and Carola Wenk. Clustering trajectories for map construction. In *Proceedings of the 25th ACM SIGSPATIAL International Conference on Advances in Geographic Information Systems*, SIGSPATIAL '17, 2017. doi:10.1145/3139958.3139964.
- [7] Kevin Buchin, Maike Buchin, Joachim Gudmundsson, Jorren Hendriks, Erfan Hosseini Sereshgi, Vera Sacristán, Rodrigo I. Silveira, Jorrick Sleijster, Frank Staals, and Carola Wenk. Improved map construction using subtrajectory clustering. In *LocalRec'20: Proceedings of the 4th ACM SIGSPATIAL Workshop on Location-Based Recommendations, Geosocial Networks, and Geoadvertising, LocalRec@SIGSPATIAL 2020, November 3, 2020, Seattle, WA, USA*, pages 5:1–5:4, 2020. doi:10.1145/3423334.3431451.
- [8] Kevin Buchin, Maike Buchin, Joachim Gudmundsson, Maarten Löffler, and Jun Luo. Detecting commuting patterns by clustering subtrajectories. *International Journal of Computational Geometry and Applications*, 21(3):253–282, 2011. doi:10.1142/S0218195911003652.
- [9] Maike Buchin, Bernhard Kilgus, and Andrea Kölzsch. Group diagrams for representing trajectories. *International Journal of Geographical Information Science*,

- 34(12):2401–2433, 2020. doi:10.1080/13658816.2019.1684498.
- [10] Maike Buchin and Carola Wenk. Inferring movement patterns from geometric similarity. *J. Spatial Inf. Sci.*, 21(1):63–69, 2020. doi:10.5311/JOSIS.2020.21.724.
- [11] Mark de Berg, Atlas F. Cook, and Joachim Gudmundsson. Fast Fréchet queries. *Computational Geometry*, 46(6):747–755, 2013. doi:https://doi.org/10.1016/j.comgeo.2012.11.006.
- [12] Anne Driemel, Sariel Har-Peled, and Carola Wenk. Approximating the Fréchet distance for realistic curves in near linear time. *Discrete & Computational Geometry*, 48(1):94–127, 2012. doi:10.1007/s00454-012-9402-z.
- [13] Joachim Gudmundsson and Nacho Valladares. A GPU approach to subtrajectory clustering using the Fréchet distance. *IEEE Trans. Parallel Distributed Syst.*, 26(4):924–937, 2015. doi:10.1109/TPDS.2014.2317713.
- [14] Joachim Gudmundsson and Sampson Wong. Cubic upper and lower bounds for subtrajectory clustering under the continuous Fréchet distance, 2021. doi:10.48550/ARXIV.2110.15554.
- [15] Catalin Ionescu, Dragos Papava, Vlad Olaru, and Cristian Sminchisescu. Human3.6m: Large scale datasets and predictive methods for 3d human sensing in natural environments. *IEEE transactions on pattern analysis and machine intelligence*, 36(7):1325–1339, 2013. doi:10.1109/TPAMI.2013.248.
- [16] Björn Krüger, Anna Vögele, Tobias Willig, Angela Yao, Reinhard Klein, and Andreas Weber. Efficient unsupervised temporal segmentation of motion data. *IEEE Transactions on Multimedia*, 19(4):797–812, 2017. doi:10.1109/TMM.2016.2635030.
- [17] Jae-Gil Lee, Jiawei Han, and Kyu-Young Whang. Trajectory clustering: a partition-and-group framework. In *Proceedings of the ACM SIGMOD International Conference on Management of Data, Beijing, China, June 12-14, 2007*, pages 593–604, 2007. doi:10.1145/1247480.1247546.
- [18] Lily Lee and W Eric L Grimson. Gait analysis for recognition and classification. In *Proceedings of Fifth IEEE International Conference on Automatic Face Gesture Recognition*, pages 155–162. IEEE, 2002.
- [19] Rick Lumpkin and Luca Centurioni. Global drifter program quality-controlled 6-hour interpolated data from ocean surface drifting buoys. NOAA National Centers for Environmental Information, 2019. doi:10.25921/7ntx-z961.
- [20] Jana Mattheus, Hans Grobler, and Adnan M. Abu-Mahfouz. A review of motion segmentation: Approaches and major challenges. In *2020 2nd International Multidisciplinary Information Technology and Engineering Conference (IMITEC)*, pages 1–8, 2020. doi:10.1109/IMITEC50163.2020.9334076.
- [21] C MoCap. Carnegie mellon university graphics lab motion capture database, 2007. URL: <http://mocap.cs.cmu.edu/>.
- [22] Sen Qiao, Y. Wang, and J. Li. Real-time human gesture grading based on OpenPose. *2017 10th International Congress on Image and Signal Processing, BioMedical Engineering and Informatics (CISP-BMEI)*, pages 1–6, 2017. doi:10.1109/CISP-BMEI.2017.8301910.
- [23] Petr Slavík. A tight analysis of the greedy algorithm for set cover. In *Proceedings of the twenty-eighth annual ACM symposium on Theory of computing*, pages 435–441, 1996.
- [24] Roniel S. De Sousa, Azzedine Boukerche, and Antonio A. F. Loureiro. Vehicle trajectory similarity: Models, methods, and applications. *ACM Comput. Surv.*, 53(5), September 2020. doi:10.1145/3406096.
- [25] Erik van Sebille, Stephen M. Griffies, Ryan Abernathy, Thomas P. Adams, Pavel Berloff, Arne Biastoch, Bruno Blanke, Eric P. Chassignet, Yu Cheng, Colin J. Cotter, Eric Deleersnijder, Kristofer Döös, Henri F. Drake, Sybren Drijfhout, Stefan F. Gary, Arnold W. Heemink, Joakim Kjellsson, Inga Monika Koszalka, Michael Lange, Camille Lique, Graeme A. MacGilchrist, Robert Marsh, C. Gabriela Mayorga Adame, Ronan McAdam, Francesco Nencioli, Claire B. Paris, Matthew D. Piggott, Jeff A. Polton, Siren Rühls, Syed H.A.M. Shah, Matthew D. Thomas, Jinbo Wang, Phillip J. Wolfram, Laure Zanna, and Jan D. Zika. Lagrangian ocean analysis: Fundamentals and practices. *Ocean Modelling*, 121:49–75, 2018. URL: <https://www.sciencedirect.com/science/article/pii/S1463500317301853>, doi: <https://doi.org/10.1016/j.ocemod.2017.11.008>.
- [26] Sheng Wang, Zhifeng Bao, J Shane Culpepper, and Gao Cong. A survey on trajectory data management, analytics, and learning. *ACM Computing Surveys (CSUR)*, 54(2):1–36, 2021. doi:10.1145/3440207.
- [27] Guan Yuan, Penghui Sun, Jie Zhao, Daxing Li, and Canwei Wang. A review of moving object trajectory clustering algorithms. *Artificial Intelligence Review*, 47(1):123–144, 2017. doi:10.1007/s10462-016-9477-7.
- [28] Feng Zhou, Fernando De la Torre, and Jessica K Hodgins. Hierarchical aligned cluster analysis for temporal clustering of human motion. *IEEE Transactions on Pattern Analysis and Machine Intelligence*, 35(3):582–596, 2012.

## A Additional Figures

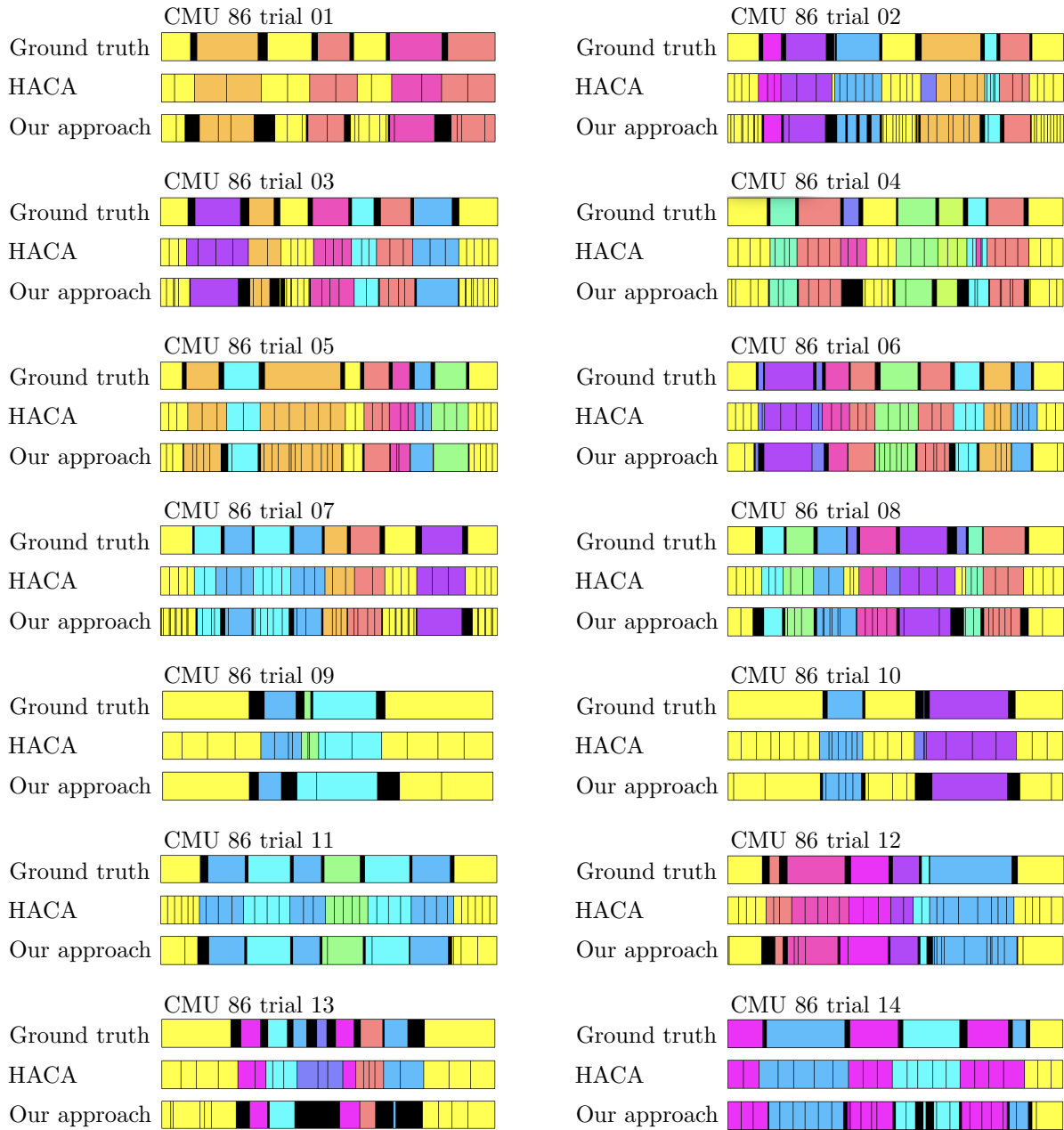


Figure 10: Segmentation result of subtrajectory clustering on CMU data. Black bars within the ground truth labeling correspond to a transition between labels. Thin black lines in the HACA labeling and our labeling correspond to a segmentation within a single label, while fat black lines in our labeling indicate uncertainty, that is that point along the trajectory could be in one of multiple labels.

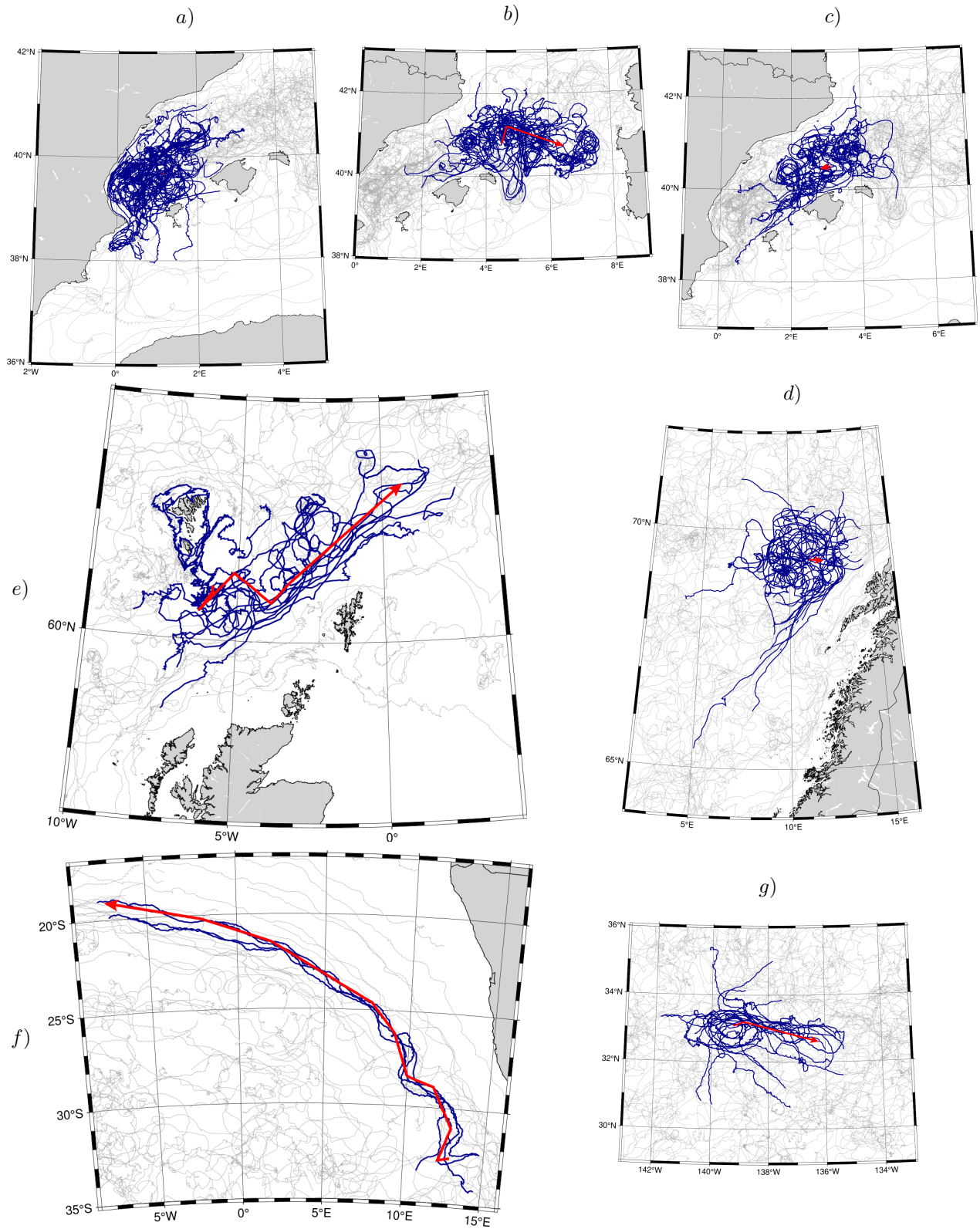


Figure 11: The first seven cluster centers (red) and their approximate coverage (blue) selected during the greedy SETCOVER algorithm on the Global Drifter Program Data with  $\Delta = 15\text{km}$  and  $l = 10$ .

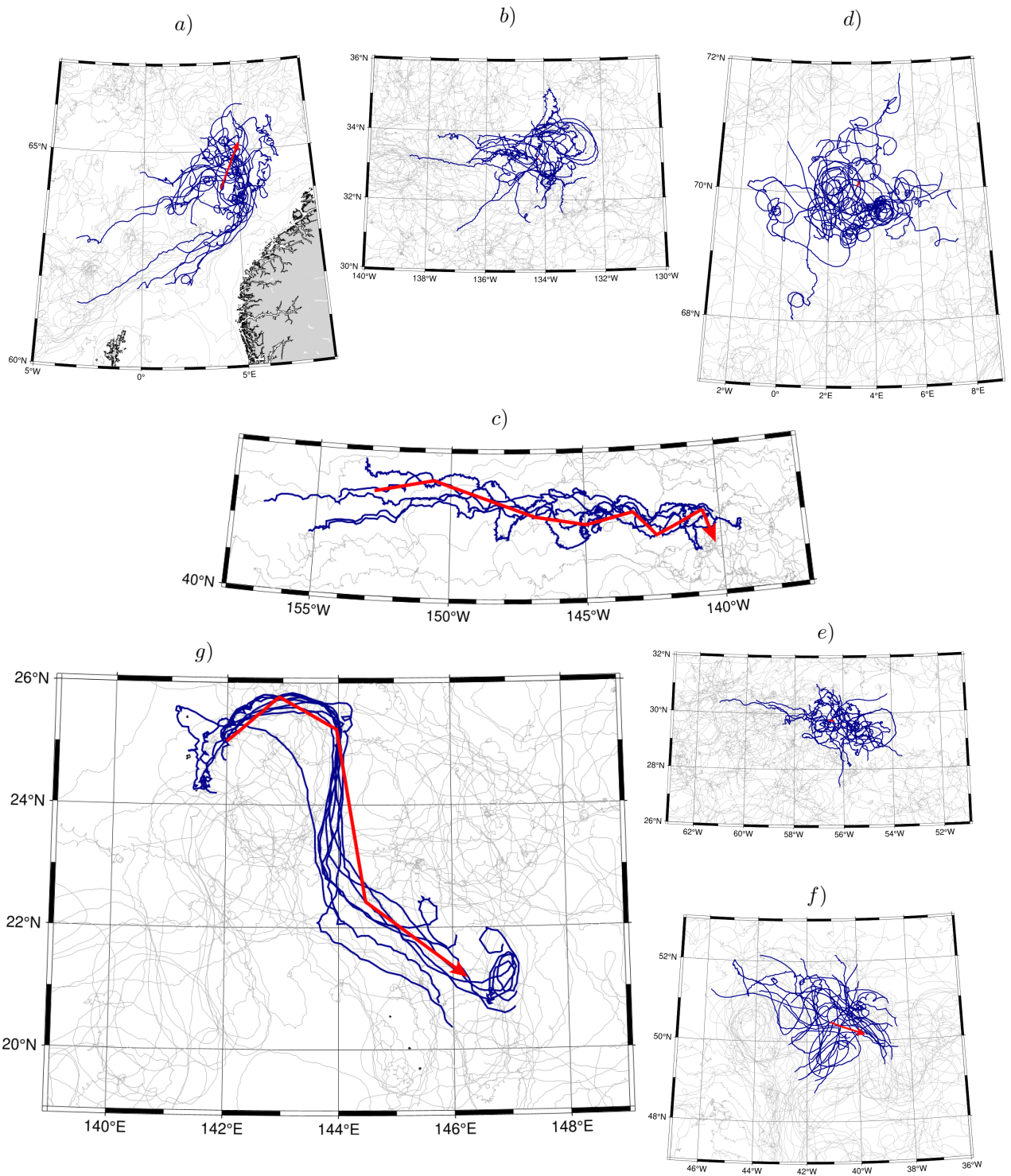


Figure 12: The eight to fourteenth cluster centers (red) and their approximate coverage (blue) selected during the greedy SETCOVER algorithm on the Global Drifter Program Data with  $\Delta = 15\text{km}$  and  $l = 10$ .

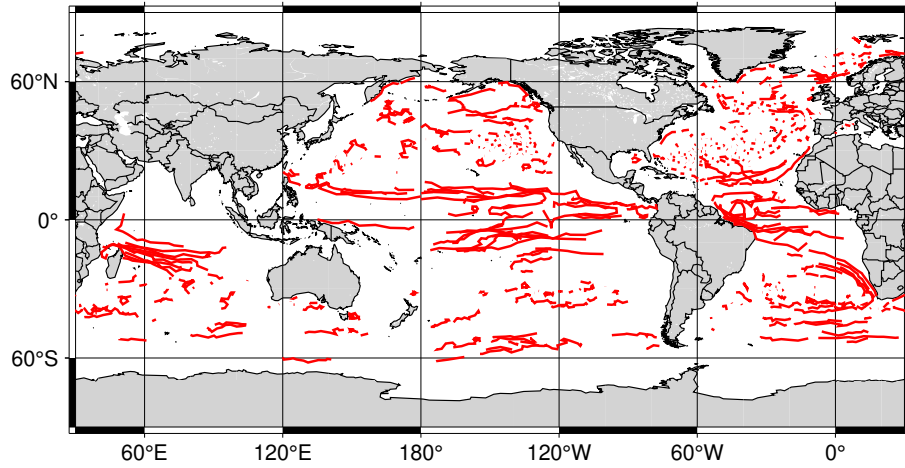


Figure 13: First 500 cluster centers computed by our algorithm with  $\Delta = 15\text{km}$  and  $l = 10$ . These can be visually compared with the main underlying ocean currents according to experts shown in Figure 15.

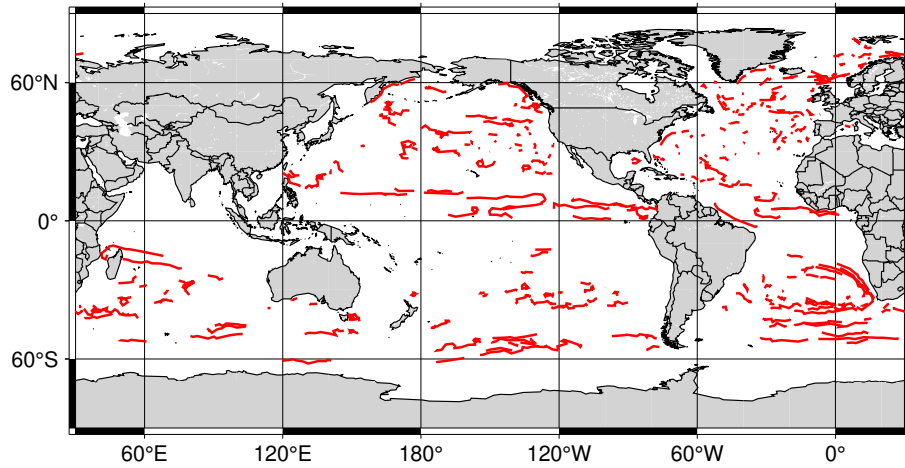


Figure 14: The same cluster centers as shown in Figure 13, but with cluster centers consisting of a single edge or whose coverage consists of only one subtrajectory filtered out.

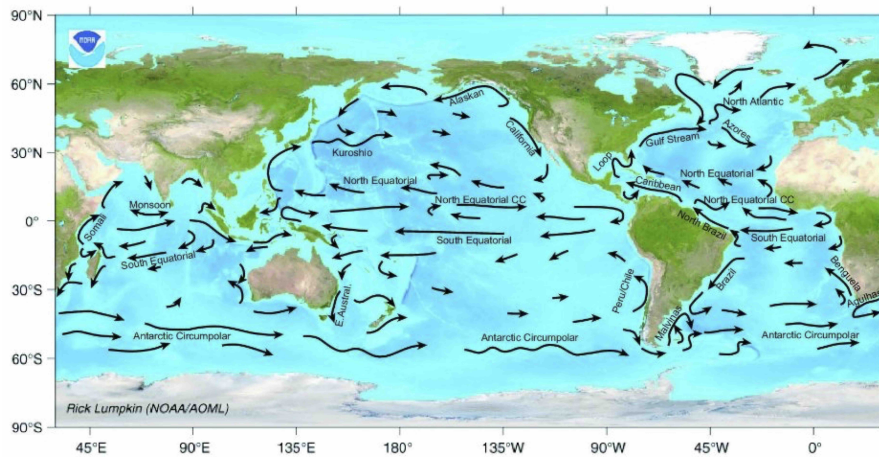


Figure 15: Schematic map of major ocean currents. Source: Rick Lumpkin (NOAA/AOML).